Design and Analysis of a Formula Student Carbon Fibre Rim

K. Korntved, J. Hersbøll, M. Lauritsen, K. Bording, H. Leto

Department of Materials and Production, Aalborg University
Fibigerstraede 16, DK-9220 Aalborg East, Denmark
Email: (kkornt13, jhersb12, mlau13, kbordi12, hleto13)@student.aau.dk,
Web page: http://www.mechman.m-tech.aau.dk/

Abstract
This article deals with weight minimization of the rims of a Formula Student race car for the AAU Racing team. This was accomplished by switching from aluminium to carbon fibre composite material, and using two different approaches for determining the number of layers and their respective orientation. Initially the loads acting on the rim are defined by usage of a dynamic model of the race car. These loads are then validated through stresses obtained from FEA on a stock aluminium rim. The first approach for determining the layup is initially inspired by the principle stress directions of the aluminium rim, and then iteratively improved by considering the failure modes of the layers, and altering the layup accordingly. The second approach consists of an optimization algorithm, constrained to a symmetric and balanced layup, which minimizes the weight while not violating the failure indexes. These two layups are subsequently analysed in various load cases and modified to remain within the requirements. The final result is a 51 % reduction in weight compared to the reference aluminium rim.

Keywords: Keywords: rim, formula student, race car dynamics, composite materials, fibre angle optimization, finite element analysis, optimization

1. Introduction

In race car applications weight is often considered a critical factor in the search for performance increase. This paper focuses on the redesign of a 10 inch rim for a FSAE race car at Aalborg University, using a carbon fibre reinforced material to reduce the overall weight of the race car. A commercial aluminium rim geometry is adopted for an initial model. This geometry poses a rim made in two pieces, illustrated in figure 1, manufactured by Keizer [1].

The primary goal of a redesign is to optimize the weight, without compromising structural performance. Two composite rim designs are considered. One design is based on intuitive engineering design analysis and another design is based on optimization synthesis using generic and direct search algorithms. Pros and cons of the models are assessed, to discuss which one has the lowest weight and provides the highest strength and stiffness, while they are furthermore evaluated on time consumption for the design process.

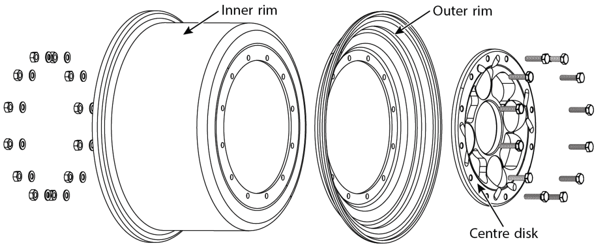

Fig. 1 Aluminium rim sub-structured.

2. Load Determination

To determine loads of the wheel, a dynamical model for the AAU race car is established. Through this model, some assumptions are taken for simplification. These are considered conservative and are supported in the main report [2]. The model is based on dynamical equilibrium equations and takes into account effects of acceleration, braking and turning, as well as the self-weight and downforce.

The highest loads are considered as a combination of braking and turning, which occurs simultaneously when driving with high speed through a curve. The normal force is calculated in contributions from self-weight, downforce, longitudinal acceleration and lateral acceleration. Free Body Diagrams (FBD) from these contributions, with added length notations, are illustrated in Fig. 2 and Fig. 3. Illustrations are for braking and left turning, thus a_x changes direction for acceleration.

of this would be mostly concentrated on 80% of the full contact patch [4].

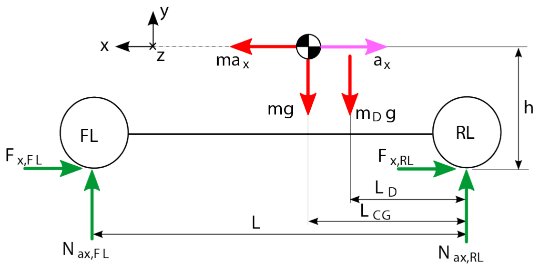

Fig. 2 FBD of contribution from self-weight and longitudinal acceleration, during braking and left turn. Front left tyre is notated FL and rear left tyre is notated RL.

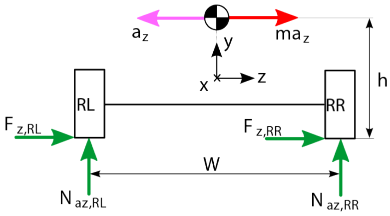

Fig. 3 FBD of contribution from lateral acceleration, during braking and left turn. Rear left tyre is notated RL and rear right tyre is notated RR.

Forces found from braking through a left turn, i.e. shifting the highest loads to the front right (FR) tyre, are considered load case one in Tab. I. Three additional load cases are considered. These include maximum braking (Load case 2), maximum left turning (Load case 3), and combined right turning and braking (Load case 4). Additional load cases are likewise applied to the front right (FR) tyre.

	a_x [m/s^2]	a_z [m/s^2]	N_{FR} [N]	$F_{x,FR}$ [N]	$F_{z,FR}$ [N]
Load case 1	1.0g	1.6g	1900	-1400	-2300
Load case 2	0g	2g	1500	-3100	0
Load case 3	2.5g	0g	1700	0	-2800
Load case 4	1.0g	-1.6g	500	400	-600

Tab. I Forces acting on the front right (FR) wheel, during the four load cases. Tabled accelerations are data provided from the AAU Racing Team [3]. Forces are rounded off.

2.1 Validation

To verify loads obtained from the dynamic model, the Finite Element Method (FEM) is used to compare the maximum found von Mises yield stress to the yield strength of a stock 10 inch aluminium rim. Specifics on parameters of the aluminium rim and setup of the Finite Element Analysis (FEA) is given in the main report [2], but loaded areas are briefly introduced in the following. Two contact patches has been determined, Fig. 4, one spanning 25 degrees and a smaller contact patch of 20 degrees is used for the normal force, as the distribution of this would be mostly concentrated on 80% of the full contact patch [4].

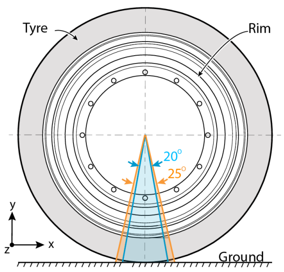

Fig. 4 Contact patches of 20 and 25 degrees, illustrated on an undeformed rim and tyre.

These contact patches span the full width of the rim and determined forces are applied as couples, to model the rim without tyre. The loading scenario is set up for the front right (FR) wheel, exposed to a simultaneous cornering and braking condition, which is considered the most loaded scenario. Application of forces is illustrated in Fig. 5.

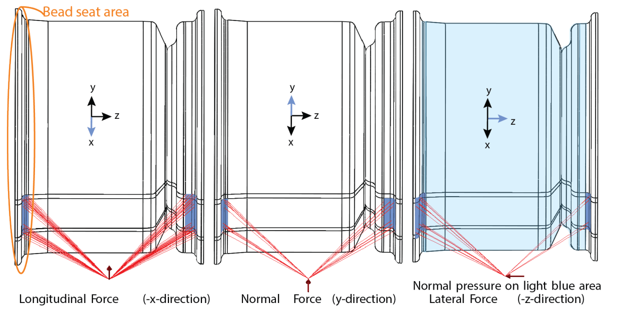

Fig. 5 Three different force components (blue faces) and one pressure (Light blue faces) applied to the rim.

FEA shows that the rim is subjected to a maximum Von Mises converged reference value of 330 MPa. This value is in the area of lateral and normal load introduction on the bead seat of the rim.
Comparing 330 MPa to the yield strength of the aluminium material, there is a 16.5% margin. It is a relatively small margin, but considering that the dynamic model is conservative in determination of the loads, it is considered acceptable.

3. Selection of Safety Factor

Due to uncertainties on the maximum loads during operation, a safety factor is considered appropriate. Likewise, uncertainties w.r.t. the composite material is considered, since the strength parameters can be affected by e.g. ply-drops, moisture and heat. The chosen safety factor is composed of several partial coefficients, as

suggested in [5], and the result is $\gamma_m = 1.40$.
Since failure criteria, related to composite materials, are expressed in terms of failure indices FI, the safety factor γ_m is converted to failure indices, by calculating the reciprocal value:

$$FI = \frac{1}{1.40} = 0.714 \quad (1)$$

4. Dynamic Response

The dynamic response of the rim during operation must be taken into account. Specifically it must be checked, whether the operational frequency of the system is below one third of the fundamental eigenfrequency, i.e.

$$\omega_{max} \leq \frac{1}{3}\omega_0 \quad (2)$$

If the above requirement is satisfied, it is sufficient to perform a static failure analysis of the rim. Since the top speed of the race car is 170 km/h (47.22 m/s) [3], this number can be converted into the operational frequency of the wheel as:

$$\omega_{max} = \frac{v_{max}}{r} = 205.3rad/s = 32.7Hz \quad (3)$$

Thus the fundamental eigenfrequency of the composite rim must be above three times the operational frequency, i.e. $3 \cdot 32.7Hz = 98.0Hz$.

5. Requirements

To asses a final composite rim design, requirements are defined and explained in the main report [2]. The most important requirements are listed below:

- Minimum weight reduction of 1 kg.
- Rim must withstand loads in table I.
- Failure index < 0.714.
- Minimum natural frequency of 98 Hz.

6. Materials and Manufacturing

Two types of carbon fibre prepregs are available from Terma A/S for the rim design, which are:

- UD (IM7-12K)
- Twill (IM7-6K-5HS)

As plotted in Fig. 6, properly angled UD provides very high stiffness compared to twill and aluminium.

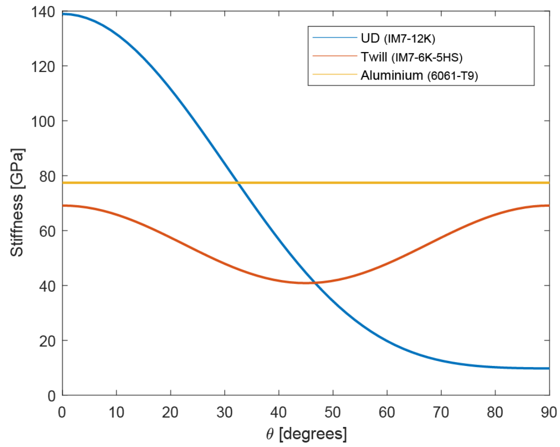

Fig. 6 Stiffness as a function of fibre angle, for UD, twill and aluminium.

Autoclaving is selected as the manufacturing method, since this provides good product quality, especially for composites with high fibre content, which is the case for the available prepregs.

7. Failure Criteria

Failure criteria are generally used to assess the strength a composite layup. It is chosen to make use of two failure criteria in this paper, as failure of composites can be very complicated. This means that failure criteria for composite materials does not always yield accurate results. The chosen criteria are the maximum stress criterion and the Tsai-Wu criterion. For both criteria, the following in-plane strength parameters are used:

X_t	Tensile strength in longitudinal fibre direction
X_c	Compressive strength in longitudinal fibre direction
Y_t	Tensile strength in transversal fibre direction
Y_c	Compressive strength in transversal fibre direction
S	In-plane shear strength

7.1 Max Stress Failure Criterion

This criterion is based on the inequality between applied stress or strain in principal material coordinates and the related strength. The criterion relies on the assumption, that a lamina is subjected to failure, if strains or stresses exceeds the maximum strength for a specific direction. Mathematically this is expressed by:

$$\begin{aligned}
&\text{For } \sigma_i > 0: \quad FI_1 = \frac{\sigma_1}{X_t} \quad FI_2 = \frac{\sigma_2}{Y_t} \quad FI_3 = \frac{|\sigma_{12}|}{S} \\
&\text{For } \sigma_i \leq 0: \quad FI_1 = \frac{\sigma_1}{X_c} \quad FI_2 = \frac{\sigma_2}{Y_c} \quad FI_3 = \frac{|\sigma_{12}|}{S} \quad (4) \\
&max(FI_1, FI_2, FI_3) \leq 0.714
\end{aligned}$$

The advantage of this criterion is the ease of usage and prediction of the actual failure modes. The drawback is, that it does not take interaction between different failure modes into account.

7.2 Tsai-Wu Failure Criterion

The Tsai-Wu criterion is a polynomial failure criterion, which has the following compact form:

$$F_i\sigma_i + F_{ij}\sigma_i\sigma_j \leq 0.714 \qquad i,j = 1,2,...,6 \quad (5)$$

where F_i and F_{ij} are constants containing the strength parameters. The advantage of the Tsai-Wu criterion is, that it accounts for interaction effects. However the accuracy of the criterion depends on the applied mixed term F_{12}, which has to be determined experimentally for providing an accurate value. Since this is very difficult, the default value in Ansys [6] is selected. The largest failure index is chosen as the largest value obtained from these two criteria.

8. Intuitive Engineering Approach

The approach focuses on an intuitively engineered design of a composite rim. In this approach fibre orientations and thickness are altered manually for improving the design in an iteratively manner.

It is chosen to apply a combination of UD and twill weave to both provide tailored stiffness properties from UD and flexibility for better draping properties from twill. Additionally it is chosen to apply symmetric laminates. This eliminates bending-extension stiffness coupling, by which warping of the laminate during curing is avoided.

Before the intuitive engineering approach is conducted, preliminary work is necessary before advancing straight into the modelling process. Preliminary work includes considerations and choices on geometry and element formulation, as well as general knowledge on initial fibre layup.

8.1 Preliminary Work

The original Keizer rim geometry has a varying thickness, which is not well suited for shell modelling. Thus the geometry is modified for the highlighted areas in Fig. 7.

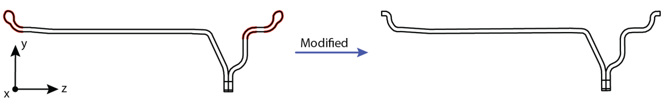

Fig. 7 Section cut of the upper half of the rim. The Keizer original geometry is to the left, and the modified geometry, with a constant thickness, is to the right.

For discretization of the model, three types shell elements for layered structures have been considered, namely SHELL181, SHELL281, and SOLSH190. These are all suitable for analysing thin to moderately thick shell structures [6]. A benchmark test of all three elements on the modified rim geometry is collected in the main report [2]. It was decided to use SHELL181 and SHELL281, even though the solid shell (SOLSH190) showed good results. This is because using SOLSH190 requires a lot of extra programming. Shell181 is a linear six degrees of freedom element type, which is advantageous when the thickness of the model is increased numerous times, during the design process. For the optimization approach, the better quadratic SHELL281 is used, as the thickness is only decreased with the optimization approach, thus not violation of the kinematic assumptions is expected.

8.2 Composite Layup

When working with layered composites, multiple layers of fibres are needed, to achieve desired strength and stiffness. The general thoughts on orienting fibres are based upon change in principle stress directions. Furthermore, principal stress directions, as well as the concentration of strain energy density and change in curvature of the geometry, is considered to divide the geometry into sections. In Fig. 8, looking at especially the inner rim bead seat, both compressive stresses (blue vectors) and tensile stresses (red vectors) are present around the circumferential. It is important to note that the rim rotates, which means that some areas are exposed to both compressive and tensile stress during rotation.

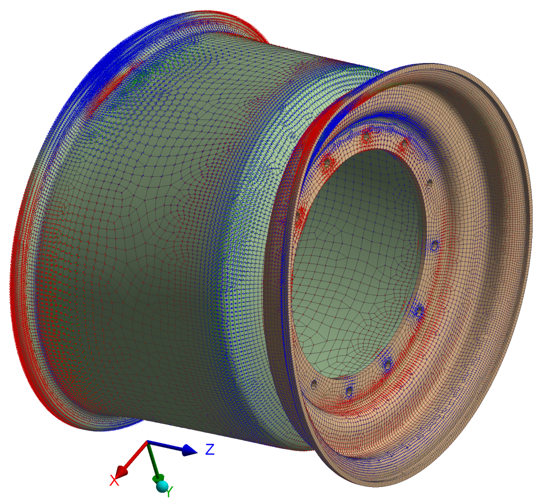

Fig. 8 Principal directions of stresses represented by scaled vectors.

The rim is subdivided into eight sections. These sections are illustrated in Fig. 9. The sections are chosen based on above discussion. Especially rapid changes in principal stress directions and geometry defines where to add sections.

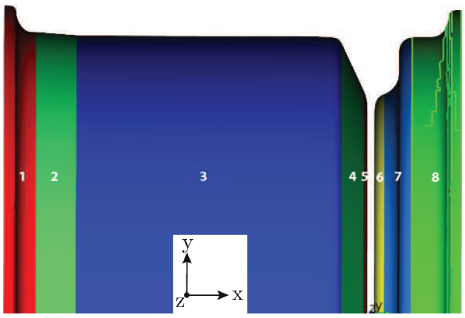

Fig. 9 Chosen layup sections.

8.3 Intuitive Engineering Analysis

A simple initial model is created, where quasi-isotropic stacks are layered until neither the Tsai-Wu or max stress criterion show a failure index above 0.714, as was calculated in equation (1). From this initial model, iterative design changes are made until a satisfying weight of the rim is achieved, while satisfying the requirements. This process is shown in Fig. 10.

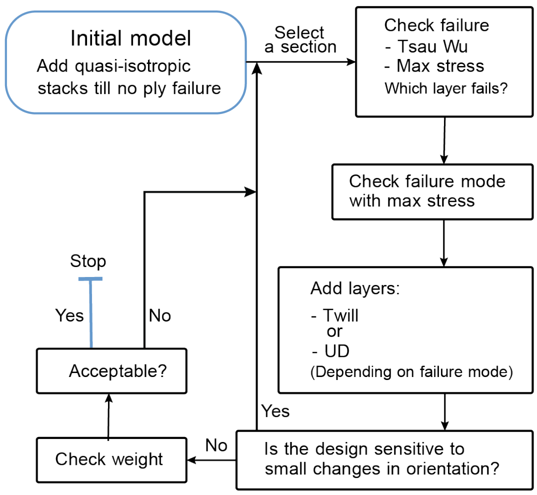

Fig. 10 Flowchart for the work flow in the intuitive engineering approach. This iteration is repeated for all of the rim sections.

8.4 Results

With the final intuitively engineered design, a weight of 727 grams is obtained, having a maximum failure index of 0.715. As this is not the final rim result, the failure index is allowed to exceed the maximum failure index initially decided upon.
Note that the failure index is the largest failure index of the two criteria - in this case Tsai-Wu.

9. Optimization Approach

The optimization approach takes basis in formulating the objective function as the weight dependant on the fibre orientations and the number of layers in each section.
Only UD is applied in the optimization in order to reduce the number of design variables, such that only fibre orientations and number of plies are varied.
To further reduce the number of design variables it is chosen to apply both symmetric and balanced layup. With this type of layup all coupling effects are eliminated.

9.1 Formulation of the problem

In order to reduce the number of variables as much as possible the fibre orientations and number of layers are incorporated as dependant variables of a single independent variable x, which is defined between -1 and 1. The variables are defined as:

$$\begin{cases} -1 \leq x < 0: & t = 0 \quad \bigwedge \quad \theta = 0 \\ 0 \leq x \leq 1: & t = 0.13\text{mm} \quad \bigwedge \quad \theta = 180x - 90 \end{cases} \tag{6}$$

With the above formulation and the application of symmetric and balanced laminates the total number of design variables in the problem sums up to the number of sections in the FE-model multiplied with one quarter of the number of layers.
The constraint for the problem is, that the Tsai-Wu and maximum stress failure indeces must be below 0.714 as stated earlier. The requirement regarding the natural frequency as well as the other load cases are not included in the optimization formulation but is checked in a subsequent post-analysis.

9.2 Selection of Algorithm

The selection of optimization method is based on several criteria. The optimization problem is highly non-convex, and thus a method, which can cope with this issue is needed. Furthermore the convergence time is very important, since a high DOF and time consuming FEA must be run in each iteration. Therefore two algorithms are initially investigated. These are the genetic algorithm, which is advantageous for non-convex problems, and the pattern search, which in general has fast solution time but has the disadvantage, that it can only converge into local minima. The searching principles of these algorithms are briefly illustrated in Fig. 11 and Fig. 12.

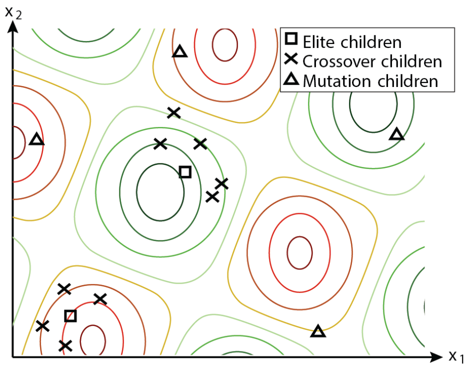

Fig. 11 Illustration of the searching principle of the genetic algorithm by use of different searching agents called children. The chart illustrates several local minima (smallest circles), which is what the elite children are good at finding. Crossover children are searching the nearby space of the elite children and mutation children search more wide and helps to widen the search space, such that the algorithm is less sensitive to local minimums.

From each iteration of the pattern search, the base point moves closer to a minimum and the exploratory search space increases, which is done for a faster converge to the minimum. This is true for search one to three. For search 4, the base point remains the same and the search space halves, to get closer to the minimum.

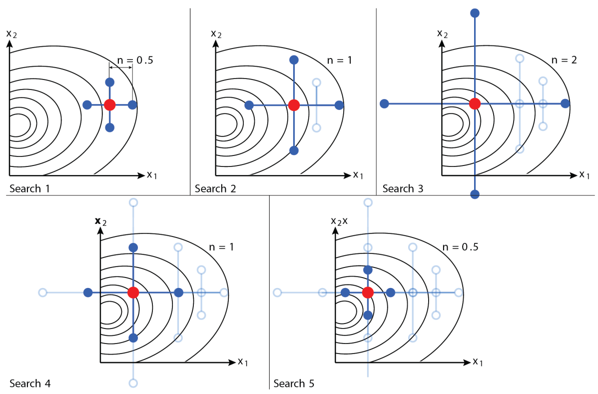

Fig. 12 5 steps of the pattern search iteration process. The principle is, that one center point and a couple of adjacent points of each design variable is evaluated through the objective function. From this information the best set of design variables is selected for the next iteration, and the step size is doubled. If the middle point contains the best set, the step size is halved instead for searching more locally.

9.3 Optimization Program

The selected algorithms are implemented in a MATLAB optimization program, for which the structure is shown in Fig. 13.

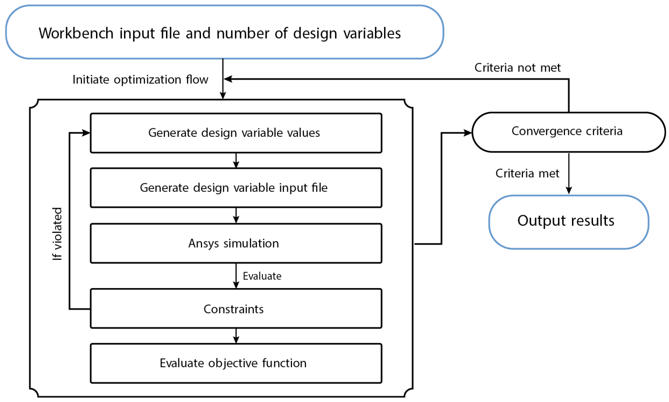

Fig. 13 Structure of the optimization program.

The principle in the program is briefly presented in the following. Initially an ANSYS Workbench input file containing the discretized rim model is called in the program, from which an ANSYS APDL input file is generated based on an initial guess on the design variables, which are initially specified in the program. Next the Ansys simulation is run, constraints are checked and the objective function is evaluated. Then a new set of design variables are created based on information of the objective function values. Between each iteration a convergence criterion is evaluated, which states that if the best design objective is not changed within 5 iteration, the algorithm stops and outputs the results of mass, maximum deformations and maximum stress as well as Tsai-Wu failure indices.

9.4 Results

After running both optimization algorithms multiple times, the best results were obtained using the genetic algorithm. The reason for this is due to the degree of non-convexity of this optimization problem, which makes the pattern search converge to a local minimum, while the genetic algorithm explores the search space broader and thus converges to a better solution. The settings of the best trial run of the algorithm was a population of 50 and termination after 5 generations. This is far lower than the desired population size and number of generations, but these settings were chosen based on time restriction. With more time to run the optimization, a better solution can be found. After the optimization scheme has converged to a solution, the results have to be processed. Since the optimized angles determined by the design variables are continuous within the interval -90 to 90 degrees, the results are rounded to the nearest 10 degrees in order to provide more feasible numbers for the manufacturing process. Thus a final check of the failure indices are performed to make sure that the processed layup still is within the requirements.

10. Additional Considerations

Tailing the optimization analysis, subsequent analyses of the rim are carried out in order to check, that all specified requirements of the rim are satisfied. The post analysis involve checking additional load cases and the fundamental eigenfrequency. Lastly a valve hole is implemented in the geometry, and a final FEA is performed to check, that the maximum failure index is not exceeded.

10.1 Other Load Cases

Four load cases were proposed in Tab. I. The layup was changed to withstand all four load cases.
Results from the final designs obtained for each load case are presented in Tab. II.

	Load case	Failure index Tsai-Wu	Directional deformation [mm]		
			x	y	z
Intuitively engineered design	**1**	0.674	2.83	4.35	2.02
Final weight:	**2**	0.710	1.35	1.70	1.03
903 grams	**3**	0.715	2.85	4.81	2.32
	4	0.095	0.29	0.41	0.25
Optimized design	**1**	0.645	2.44	3.98	2.06
Final weight:	**2**	0.715	1.23	1.46	0.63
905 grams	**3**	0.713	2.44	4.46	2.38
	4	0.178	0.37	0.57	0.79

Tab. II Results for all load cases applied to the intuitively engineered design and the optimized design.

In order to fulfil the requirements for the additional load cases the change in the layup had to be implemented. This resulted in weight increases of both designs. The intuitively engineered design had a weight increase of 176 grams. The optimized design had a weight increase of 30 grams. The final weight of the two designs ended at 903 and 905 grams respectively.

10.2 Valve hole

A valve hole is required for inflation of the tyres. Intuition states that a valve hole should be placed in an area with low stresses, but also an area which is accessible to ease inflation of the tyre. This area is identified after checking additional load cases of the rim. The location is selected based on the distribution of the Tsai-Wu failure index, and the final location on the rim is shown in Fig. 14.

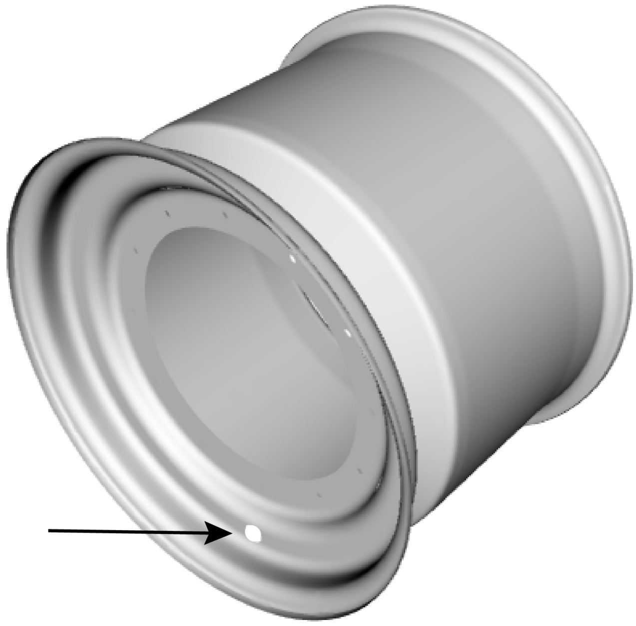

Fig. 14 Placement of the valve hole.

11. Result Comparison

The weight, maximum deformations and eigenfrequencies of the two rim designs as well as the Keizer aluminium rim are listed in Tab. III.

	Weight [gram]	Directional deformation [mm]			Natural Eigenfrequency
		x	y	z	
Keizer aluminium rim	1850	1.92	2.63	0.96	312 Hz
Intuitively engineered design	903	2.85	4.81	2.32	401 Hz
Deviation from aluminium rim	51.2%	32.6%	45.3%	58.6%	22.2%
Optimized design	905	2.44	4.46	2.38	433 Hz
Deviation from aluminium rim	51.1%	21.3%	41%	59.7%	27.9%

Tab. III Performance comparison between the two composite rim designs and the original Keizer aluminium rim.

As seen in Tab. III the weight is reduced by 51%, and the natural frequencies are increased compared to the aluminium rim. The deformations are increased, but considering the other structural parts connected to the rims (tyre/suspension system), these deformations are considered negligible.

12. Manufacturing Considerations

The manufacturing method applied for the composite rim design is the autoclave process, which is chosen as good material quality is achieved by application of both vacuum and external pressure from the autoclave.

Furthermore the process allows the usage of prepregs, where the polymer is mixed with the fibres, which ensures a good saturation of the fibres.

Since the rim is designed as two pieces, two separate moulds are needed. A proposal of the mould design is shown in Fig. 15.

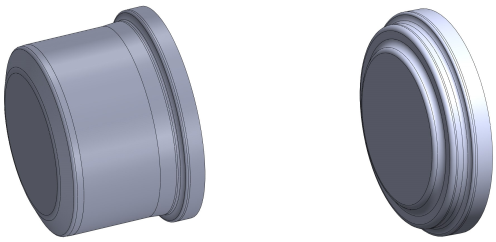

Fig. 15 Illustration of the mould for the outer rim piece.

A suggestion for how the fibre stacks should be cut into patches and laid up on the moulds can be seen in [2].

13. Conclusion

Two different designs are obtained by the the intuitive engineered design and optimized design, which have a resulting weight of 903 grams and 905 grams respectively. This correspond to a weight reduction of 51.2% and 51.1% compared to the Keizer aluminium rim respectively. The natural frequencies of both designs are improved, by which means that the dynamical response is decreased. The displacements are increased slightly compared to the aluminium rim, but these are considered negligible compared to the deformations of the whole wheel-suspension system.

Acknowledgement

The authors of this work gratefully acknowledge Sintex for sponsoring the 5th MechMan symposium. Furthermore the authors would like to thank Therma A/S for their consultation as well as the opportunity given by them to manufacture the rim.

References

[1] Keizer-Aluminum-Wheels. http://keizerwheels.com/product_cat/formula-sae-racing-wheels/, 2017. Localised 04-04-2017.

[2] K. Korntved, J. Hersbøll, M. Lauritsen, K. Bording, and H. Leto, "Design and Analysis of a Formula Student Carbon Fibre Rim," 2017.

[3] AAU-Racing. http://aauracing.dk/, 2015. Localised 02-05-2017.

[4] R. N. Jazar, Vehicle Dynamics. Springer, 1. ed., 2008.

[5] Veritas, "Standard dnv-ds-j102, design and manufacture of wind turbine blades, offshore and onshore wind turbines," Det Norske Veritas, 2010.

[6] Ansys, Ansys Documentation. SAS IP, Inc., 18.0.0 ed., 2016.